Journal of Alloys and Compounds 747 (2018) 796–802

Contents lists available at ScienceDirect

Journal of Alloys and Compounds

journal homepage: http://www.elsevier.com/locate/jalcom

Carbon coating nanostructured-$LiNi_{1/3}Co_{1/3}Mn_{1/3}O_2$ cathode material synthesized by chemical vapor deposition method for high performance lithium-ion batteries

Qian Hou [a], Gengzhen Cao [c], Peng Wang [a], Dongni Zhao [a], Xiaoling Cui [a, b], Shiyou Li [a, b], Chunlei Li [a, b, *]

[a] College of Petrochemical Technology, Lanzhou University of Technology, Lanzhou 730050, China
[b] Gansu Engineering Laboratory of Cathode Material for Lithium-ion Battery, Lanzhou 730050, China
[c] Lanzhou Petrochemical Research Center, Petrochina, Lanzhou 730060, China

ARTICLE INFO

Article history:
Received 31 January 2018
Received in revised form
8 March 2018
Accepted 9 March 2018
Available online 11 March 2018

Keywords:
Nanoscale materials
$LiNi_{1/3}Co_{1/3}Mn_{1/3}O_2$
Carbon coating
Chemical vapor deposition method
Diffusion coefficient

ABSTRACT

Efficient energy storage of lithium-ion batteries plays a significant role across lots of sectors including consumer electronics, electric and hybrid electric vehicles and a smart grid accommodating intermittent renewable energy sources. Nanostructured cathode materials present fascinating opportunities for high-performance lithium-ion batteries, but intrinsic problems linked with the high surface area to volume ratios in the nanometer-range have restricted their adoption for practical applications. We demonstrate processing platform that realize high-performance nanostructured-$LiNi_{1/3}Co_{1/3}Mn_{1/3}O_2$ (NCM) layer cathode with carbon coating as a conductive additive. In this paper, we first presented a green, novel, economic and controllable chemical vapor deposition (CVD) method with sucrose as carbon source to coating NCM. Sol-gel synthesized NCM of carbon coated with optimized thickness by this formula are shown to have outstanding rate performance and robust cycle lifetime. The thickness - optimized sample of discharge capacity is as high as 104.5 mAh g^{-1} for 10 C (6s). High capacity retentions of 94.29% and 94.78% after 100 cycles for 0.1 C, respectively. Compared with the heat evaporation method, with the CVD method has better uniformity and higher quality. This approach further improves evidently the NCM of electrochemical performance and thus promotes lithium-ion battery development technology into unprecedented regimes of operation.

1. Introduction

Efficient Electrochemical energy storage systems which can provide schemes towards a sustainable energy and globally greener future, play a decisive role in our everyday life [1–3]. At present, lithium ion batteries (LIBs) are considered the most practicable candidates for energy storage systems of portable electronic devices, electric vehicles (EV) and hybrid electric vehicles (HEV) [4–6]. Compared with $LiCoO_2$, layered-$LiNi_xCo_yMn_{1-x-y}O_2$ has attracted an increasing amount of attention as a prospective candidate cathode material for the next generation LIBs owing to its multitudinous features in terms of high capacity, thermal stability, structural stability, safety, low cost, etc [7–9]. Therefore, the layered $LiNi_{1/3}Co_{1/3}Mn_{1/3}O_2$ is believed to be one of the most reasonable candidates of the cathode materials for EV and HEV application, which can be predominantly ascribed to its high discharge capacity, low cost and excellent thermal stability of the material. It is known that $LiNi_{1/3}Co_{1/3}Mn_{1/3}O_2$ is almost zero volume or phase change when cycled among 2.50–4.40 V because the $Ni^{2+/3+/4+}$ and $Co^{3+/4+}$ redox couples provide electrochemical activity, and the inactive Mn^{4+} supplies stable framework to raise thermal stability [10,11]. In light of some previous literatures, nano-$LiNi_{1/3}Co_{1/3}Mn_{1/3}O_2$ (NCM) positive-electrode material, appropriate particles are synthesized and studied [12,13]. The particle size plays a momentous role which influences the rate capability of the positive active materials. The use of nanoscale materials is deemed to the effective way to ameliorate rate performance due to the larger contact area with electrolyte and the shorter Li^+ diffusion path [14]. That is, compared with commercial micro-particles, NCM

* Corresponding author. College of Petrochemical Technology, Lanzhou University of Technology, Lanzhou 730050, China.
E-mail address: 191348761@qq.com (C. Li).

https://doi.org/10.1016/j.jallcom.2018.03.115
0925-8388/

materials are expected to have the potential to diminish electrode polarization and improve battery capacity by the offered merits of nanostructure.

NCM integrates the features of $LiNiO_2$, $LiCoO_2$, and $LiMnO_2$. However, its electronic conductivity is relatively lower than that of $LiCoO_2$ [15]. However, low electronic conductivity in EV and HEV field is the biggest challenge for its widespread applications. In order to address the trouble, tremendous efforts have been committed, such as cation doping [16,17], surface coating [18–22], introduction of conductive agents to ameliorate the low electronic conductivity.

To improve the electronic conductivity and the electrochemical performance of NCM, carbon coating is considerable as a greatly in common used measure to improve the electronic conductivity and the electrochemical performance of NCM. An ultrathin, uniform and moderate thicknesses carbon coating of NCM applied EV and HEV is considered the sticking point for excellent long cycle life and rate performance, but it is often difficult to realize. To date, there are three major methods: the first is chemical vapor deposition (CVD) [23], the second one is traditional H_2O mixed organic compounds with NCM followed by heat evaporation (HE), the last one is the freeze drying [24]. Unfortunately, the traditional HE is very difficult to control the thickness, uniformity, conformity and composition of the coatings. In addition, it takes a lot of time by the freeze-drying method of carbon coating. For the sake of comparison, the CVD method of carbon coating has merits in terms of timesaving and simplicity. With the carbon - contained vapor flows across NCM and carbon deposited on the NCM surface, CVD is primarily considered as an effective and facile recipe to achieve uniform carbon coating. In fact, in the light of the different source offers this scheme can be divided into two types.

One hand is to use C_2H_4, CH_4 or rich-carbon gas with protective atmosphere and carrier of H_2 or N_2, and metal salts used as catalyst [25–27]. However, these gases are not environment and high cost, these introduced metal salts generally produce impurities. The other one hand is to use pyrrole monomer [28], benzene [29], methylbenzene [30] and other volatile organic liquids as carbon source carried by air or N_2 flowing. The organic compounds to be carbonized as carbon sources and flow across NCM to form conductive layers straightly [28]. However, these organic steams are generally high cost and toxicity. To address this issue, uniform carbon layer coating of the safe, effective, economic and controllable CVD is very ideal. In addition, moderate and uniform thickness of high quality carbon layer could ensure sufficiently ameliorate electronic conductivity which not mitigate the migration of Li^+ across electrode materials, which promotes lithium-ion battery development technology into unprecedented regimes of operation.

In this paper, we first presented the green, novel, economic and controllable CVD method with sucrose as carbon source and N_2 as carrier to coating NCM uniformly which were sol-gel synthesized [31]. The carbon coating NCM thus obtained are shown to have outstanding rate performance and robust cycle lifetime and outstanding rate performance even at the 10 C rate. In addition, by controlling the carbon coated weight content, the electrochemical performance of NCM was greatly improved compared with carbon coated by the traditional HE. The influence of the carbon content coating NCM of the structure and electrochemical performance is discussed explicitly.

2. Experimental section

2.1. Synthesis

The NCM powder was synthesized using Sol-gel method [32,33]. Stoichiometric amounts of Cobalt acetate $Co(CH_3COO)_2{\cdot}4H_2O$, Nickel acetate $Ni(CH_3COO)_2{\cdot}4H_2O$ and Manganese acetate $Mn(CH_3COO)_2{\cdot}4H_2O$ were used as starting materials for synthesis of the precursors. In brief, $Ni(CH_3COO)_2{\cdot}4H_2O$, $Co(CH_3COO)_2{\cdot}4H_2O$ and $Mn(CH_3COO)_2{\cdot}4H_2O$ (Co: Ni: Mn = 1:1:1) were dissolved in ethanol solution (ethanol: water = 6:4), followed by adding the acetic acid under continuous stirring at 60 °C until it became gel, and then the mixtures were preheated at 400 °C for 2 h. After that, the prepared precursors were mixed with $LiNO_3$ in the mole ratio of 1.2:1, and heated at 900 °C for 9 h.

The carbon coating NCM of preparation process is listed in Fig. 1. In Fig. 1, the CVD which was carried out in a quartz tube located horizontally. The crucible of sucrose was upstream placed close to the crucible with sol-gel synthesized NCM. The quartz tube was heated to 550 C at the speed of 10 C min^{-1} with N_2 flow of 200 cm^3 min^{-1} and maintained for 1 h. Then, the furnace was cooled with the N_2 flow. We tried to explore the ratios of 2.5:1 and 5:1 for sucrose to bare NCM (labelled by CVD1-NCM and CVD2-NCM, respectively) on the structure and electrochemical performance. In addition, the H_2O mixtures of sol-gel synthesized NCM with sucrose in 1:0.033 weight ratio was heated evaporation then placed into a tube furnace and heated to 550 C in N_2 atmosphere for 1 h

2.2. Cell preparation

As a control electrolyte, 1 M $LiPF_6$- ethylene carbonate (EC)/diethyl carbonate (DEC) (1:1) was purchased from Zhangjia-gang Guotai-Huarong New Chemical Materials Co. Ltd. The positive electrode was composed of 80 wt% NCM, 10 wt% acetylene black and 10 wt% polyvinylidene fluoride. Experimental cells (2032 type) were assembled in argon atmosphere glove box using two lithium sheets as the anode material, the above prepared electrode as the cathode material, one of the above-mentioned electrolytes as the electrolyte, and a Celgard (2400) porous polypropylene as the separator material.

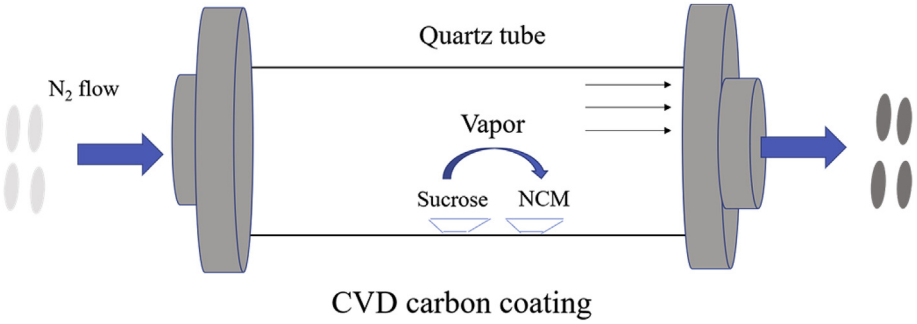

Fig. 1. Schematic illustration of the preparation process of carbon coating NCM.

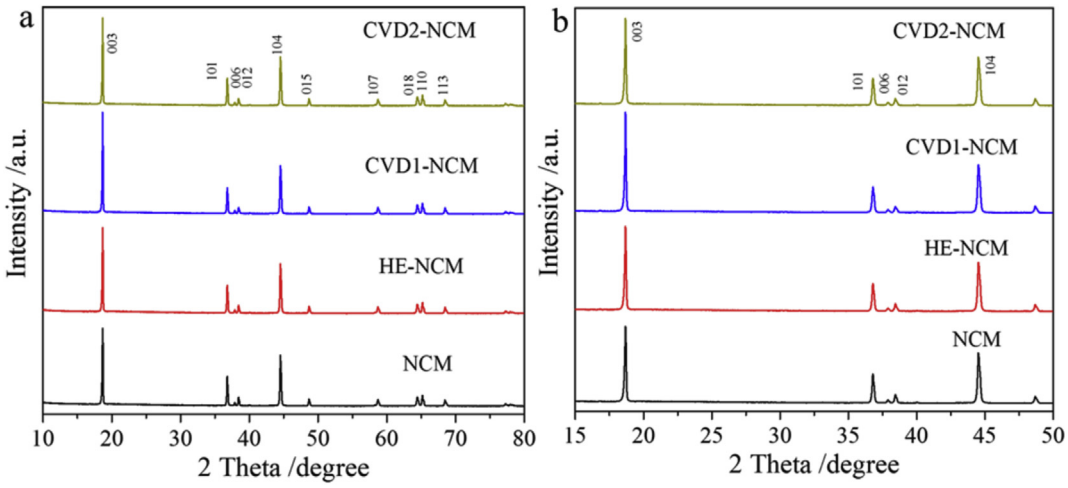

Fig. 2. The XRD patterns (a) and the zooming of main peaks (b) for sample NCM, CVD1-NCM, CVD2-NCM and HE-NCM.

2.3. Measurements

Structure characterization of the as-prepared NCM and the carbon coating NCM samples were performed by X-ray diffractometer (XRD, Rigaku, D/Max-2400) with Cu Ka radiation (40 kV, 150 mA, step size 1⁄4 0.02/s). Data were collected in the 2θ range 10–80 with a scan rate 2°/min to obtain the diffraction patterns. The morphologies were analyzed by transmission electron microscopy (TEM, JEOLJEM-1011) and high resolution trans-mission electronic microscopy (HRTEM, Tecnai G2 F20 S- Twin, FEI company, USA) The carbon content was measured by Elemental Analysis (EA) performed on a VarioEL (CHN Mode). The graphitization degree of the carbon coating was investigated by Raman spectra (Renishaw, InVia Raman Microscope).

Electrochemical measurements of cells were carried out on a LAND CT2001A tester (Wuhan, China) in the voltage range of 2.7–4.3 V at room temperature. Electrochemical impedance spectroscopy (EIS) were conducted on the electrochemical equipment CHI660D electrochemical analyzer (Shanghai Chenghua Company, China) over the frequency range from 100 kHz to 10 mHz with the amplitude of 5 mV.

3. Results and discussion

The XRD patterns of sample NCM, CVD1-NCM, CVD2-NCM and HE-NCM are presented in Fig. 2a. It is known that $LiNi_{1/3}Co_{1/3}Mn_{1/3}O_2$ has a hexagonal crystal structure of $RNaFeO_2$ with a space group of $R\bar{3}m$ [11]. The XRD patterns of all samples agree with the pattern of a pure single phase of $LiNi_{1/3}Co_{1/3}Mn_{1/3}O_2$. By virtue of zooming the main diffraction peaks (Fig. 2b), namely, (003), (101), and (104), remain at the same 2θ values for all of the samples. Additionally, no impurity phase is observed for the samples prepared in the presence of sucrose, suggesting that the structure of $LiNi_{1/3}Co_{1/3}Mn_{1/3}O_2$ is unaffected. Because the amount of carbon present on the particle is small, no diffraction peaks corresponding to the crystalline form of carbon are detected. R-factor ($R = (I_{006}+I_{102})/I_{101}$) is proportional to the hexagonal ordering, the calculated value of NCM, CVD1-NCM, CVD2-NCM and HE-NCM are 0.51, 0.5081, 0.5080 and 0.5096, which indicates the carbon coating NCM samples have higher hexagonal ordering. Additionally, the intensity ratios of $I_{(003)}/I_{(104)}$ peaks are 1.95 for CVD1-NCM, 1.96 for CVD2-NCM, 1.93 for HE-NCM and 1.92 for NCM, respectively. The higher this ratio, the lower the degree of cation mixing [8]. Generally speaking, this ratio should be larger than 1.2 for a layered compound with an outstanding electrochemical performance [34,35]. This indicates the carbon coating NCM has lower cation mixing between Li^+ and Ni^{2+}. Therefore, the low cation mixing in carbon coating NCM infers a better electrochemical performance.

Fig. 3 shows the TEM images of the bare NCM and surface-modified samples to confirm the conductive carbon coating layers on the particles surface. For the sol-gel synthesis of bare NCM (Fig. 3a) has well developed regular particles of quasi-spherical shape with a diameter distribution in the range of 100–300 nm. By contrast Fig. 3b, c and d, e, CVD1-NCM has ultrathin carbon layers about 3 nm thickness, CVD2-NCM has a little thicker carbon layer about 6 nm, according with the weight content of carbon confirmed by the EA (Table 1). In addition, there are some carbon fiber like (CF) that bridge the detached NCM particles and carbon layer that connect the neighboring particles constitute the 3D electronically conductive channels in CVD2-NCM (Fig. 3d). A good electronic conductivity, therefore, can be anticipated for the carbon coating NCM compound, which is critical for high-power application. With sharp compare, there are non-uniform thickness coatings and some free carbon could observe for sample HE-NCM with a weight content of 1.301% through a few NCM inspection, as shown in Fig. 3f and g.

Raman characterization is preferred to probe the vibrational modes of both crystalline and amorphous materials carbon coating NCM, which is shown in Fig. 4. The typical Raman spectra of CVD1-NCM and HE-NCM corresponding with $LiNi_{1/3}Co_{1/3}Mn_{1/3}O_2$ powders recorded at 632 nm excitation wavelength. The Raman active vibrations which correspond to the M–O stretching and O–M–O bending modes within MO_2 layers are generally contained between 400 and 650 cm^{-1}. The group at ~590 cm^{-1} is make up of bands at 474, 554 (Ni–O), 594 cm^{-1} (Mn–O), and 486, 596 cm^{-1} (Co–O) that represent the vibrations within the hexagonal MO_2 lattice [36,37]. Raman spectra of the CVD1-NCM and HE-NCM show intense D-band at 1343 cm^{-1} (disordered) and G-band at 1589 cm^{-1} (graphitic) bands. The D-band is ascribed to the defect-induced mode, while the G band can be associated with the tangential stretching (E_{2g}) mode of graphite. The intensity ratios of D to G peak (I_D/I_G) are calculated to be 0.988 and 1.037 for CVD1-NCM and HE-NCM, respectively, which further indicates a higher disorder degree of HE-NCM. As a result, the carbon coating with the CVD formula has a better electronic conductivity than using HE, which would have better influence on the electrochemical performance.

Fig. 5 displays the initial charge/discharge performances of bare NCM and carbon coating NCM recorded at 0.1 C. The curves

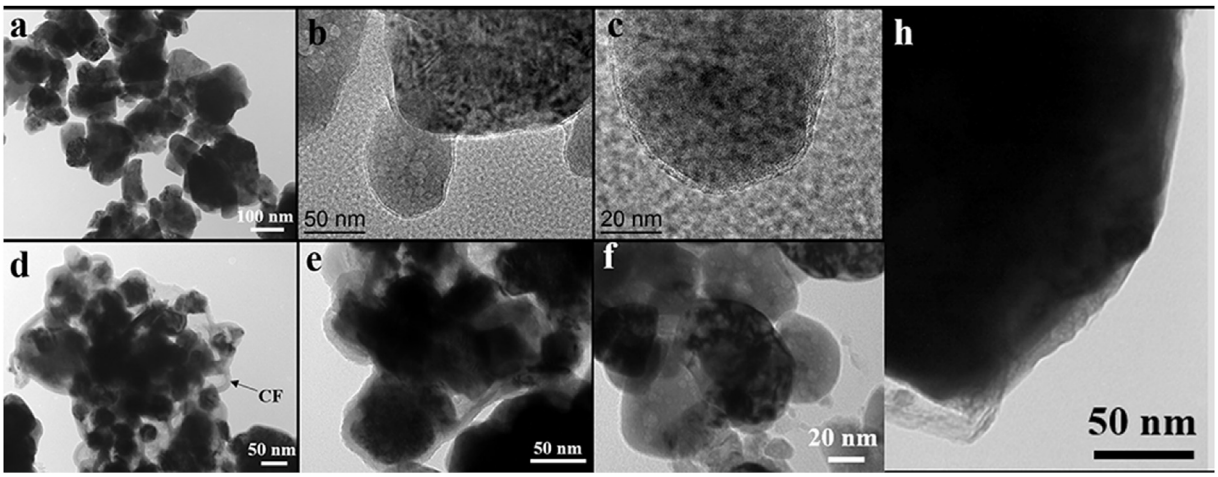

Fig. 3. TEM of NCM(a), HRTEM of CVD1-NCM (b, c), TEM of CVD2-NCM (d, e), TEM of HE-NCM (f, g).

Table 1
The carbon content of CVD1-NCM, CVD2-NCM and HE-NCM.

	CVD1-NCM	CVD2-NCM	HE-NCM
C	1.203 wt%	2.514 wt%	1.301 wt%

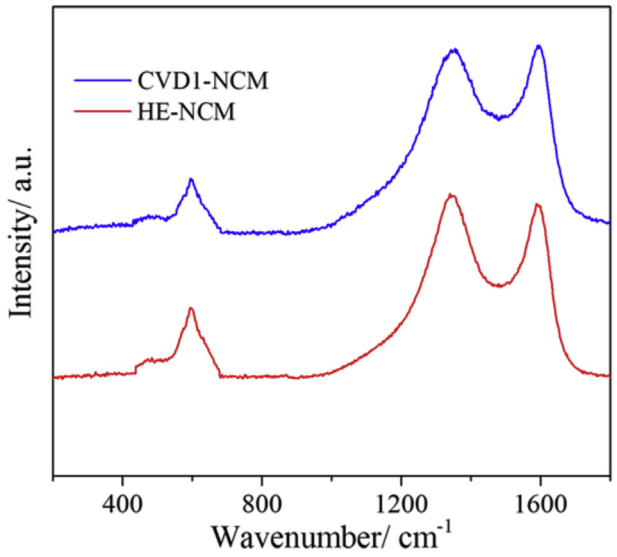

Fig. 4. Raman spectra of samples CVD1-NCM and HE-NCM.

correspond to the typical charge/discharge behavior of layered $LiNi_{1/3}Co_{1/3}Mn_{1/3}O_2$, the charge at the range of 3.75–3.90 V corresponds to the redox couple of Ni^{2+}/Ni^{3+}; the subsequent voltage ranges of 3.90–4.10 V and 4.10–4.50 V relate to the redox couples of Ni^{3+}/Ni^{4+} and Co^{3+}/Co^{4+} respectively, which is consistent with the previous reports by K. M. Shaju [38]. The initial charge capacities of bare NCM, CVD1-NCM, CVD2-NCM, HE-NCM are 223, 220.8, 218.2 and 219.9 mAh g^{-1} (2.7–4.3 V vs. Li^+/Li) at 0.1 C and the initial discharge capacities are 190.3, 207.8, 203 and 196 mAh g^{-1}, respectively. The higher specific capacity of CVD1-NCM, CVD2-NCM, HE-NCM are attributed to the lower cation mixing and the improved electronic conductivity by carbon coating. The initial columbic efficiency of bare NCM is 85.3% whereas CVD1-NCM is 94.1%, CVD2-NCM is 93%, HE-NCM is 89.1% as listed in Table 2. The

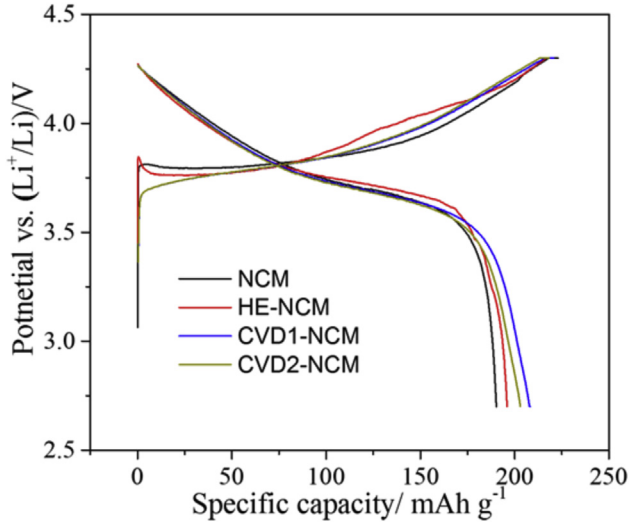

Fig. 5. Initial charge/discharge performances of NCM, CVD1-NCM, CVD2-NCM and HE-NCM.

Table 2
Simulated results for the elements of equivalent circuit.

	CVD1-NCM	CVD2-NCM	HE-NCM	NCM
R_{SEI}/Ω	2.529	2.646	2.741	3.124
R_{ct}/Ω	41.540	47.270	70.240	72.530
W/Ω	12.450	27.690	39.640	76.950
D_{Li^+}/cm^2s^{-1}	1.27×10^{-9}	8.25×10^{-10}	6.91×10^{-10}	4.76×10^{-10}

initial capacity decay was caused by SEI forming and electrolyte decomposing. The higher initial columbic efficiency of carbon coating NCM is due to the carbon coating, which inhibits the side reactions between nano-$LiNi_{1/3}Co_{1/3}Mn_{1/3}O_2$ and liquid electrolyte, leading to a reduction in the irreversible charge capacity.

Cycle performance is the basic requirement to evaluate the cathode material's performance, which is awfully crucial for the EV and HEV application. The samples of CVD1-NCM, CVD2-NCM and HE-NCM of the cycle performance at the 0.1 C are displayed in Fig. 6. The capacity retentions of bare NCM after 50 cycles is only 67.1%. However, their capacity retentions of CVD1-NCM, CVD2-NCM and HE-NCM after 100 cycles are 94.29%, 94.78% and 84.58%,

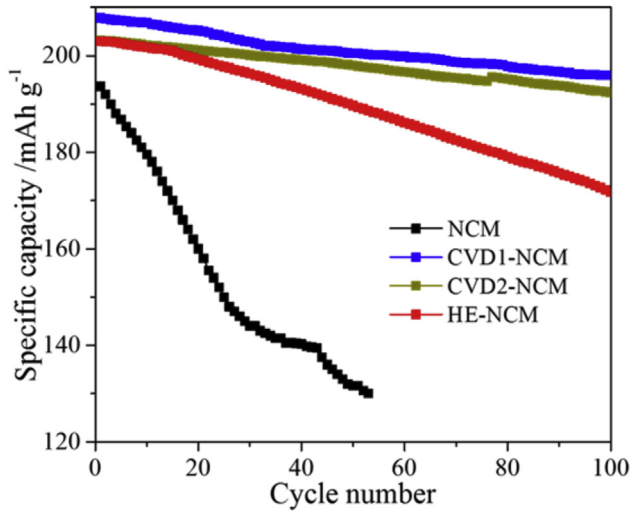

Fig. 6. Cycle performances of NCM, CVD1-NCM, CVD2-NCM and HE-NCM at 0.1 C (2.70–4.30 V).

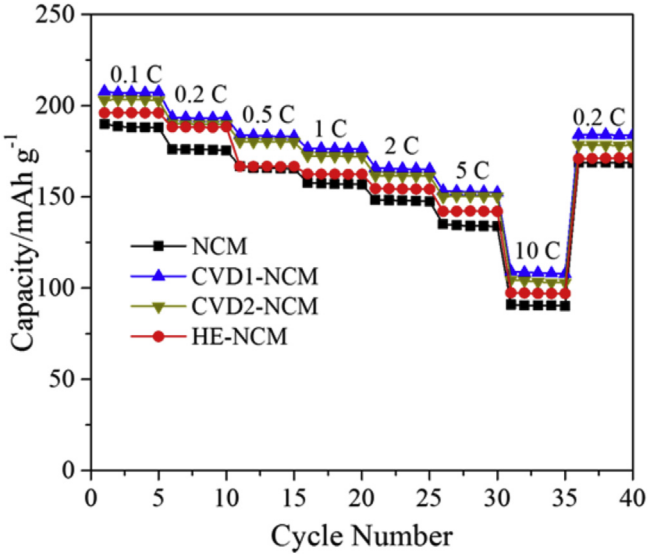

Fig. 7. Rate capabilities of NCM, CVD1-NCM, CVD2-NCM and HE-NCM from 0.1 to 10 C (2.70–4.30 V).

respectively. Sample CVD2-NCM has the highest cycle capacity retention after 100 cycles. Though the sample HE-NCM has the lowest cycle lifetime after 100 cycles, it is still fairly well.

To evaluate the effect of the weight content of sucrose to NCM and the coating formula of the rate capacity, rate performance of samples NCM, CVD1-NCM, CVD2-NCM, and HE-NCM 0.1–10C rates are displayed in Fig. 7, respectively. These samples show fairly likeness discharge capacities, for example 190.3, 207.8, 203.1 and 196.3 mAh g^{-1} at 0.1 C for samples bare NCM, CVD1-NCM, CVD2-NCM, and HE-NCM at 0.1 C, respectively. However, with the rate increased, the rate capability of these samples differently decreased. At 1 C, HE-NCM sample shows lower capacity compared with the sample of CVD carbon-coating. At 5 C, CVD2-NCM sample starts to have a lower discharge capacity than sample CVD1-NCM. These samples have quite superior high rate performance, yet. At 10 C, NCM, CVD-NCM, CVD2-NCM and HE-NCM samples have capacities of 91.1, 109 and 104.5, 97.4 mAhg^{-1}. The carbon-coating NCM samples exhibits better rate performance than NCM, which

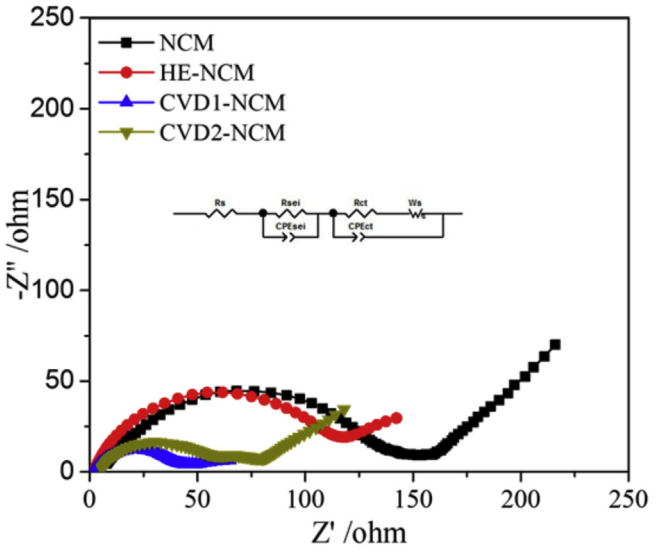

Fig. 8. Electrochemical impedance spectra (EIS) of the NCM, CVD1-NCM, CVD2-NCM and HE-NCM electrodes.

is mainly due to the coating carbon with excellent electronic conductivity, resulting in lower electrochemical impedance. The electrochemical impedance of NCM and the carbon-coating NCM were analyzed by EIS, which were conducted after the first cycle (0.1 C) at 25 °C.

EIS analysis is a formidable technology to evaluate the properties of electrode materials, in terms of conductivity, structure and charge transport in electrode materials/electrolyte interface. The Nyquist plots of the discharged bare NCM, CVD1-NCM, CVD2-NCM, and HE-NCM at the first cycle were obtained using EIS as shown in Fig. 8. In the fitted equivalent circuit, the semicircle in the high frequency range represented typically be ascribed to the resistance of a solid-state interface layer formed on the electrode surface (R_{SEI}), and the semicircle observed in the medium-to-low frequency range was contributed to charge transfer resistance (R_{ct}) between the electrode and electrolyte. Moreover, the sloping line at low frequency region is the Warburg impedance (W), which is related to the lithium ions diffusion through the solid electrode [39]. Samples CVD1-NCM has the lowest R_{SEI} and R_{ct}, however, NCM has highest R_{SEI} and R_{ct}, respectively, as outlined in Table 2. Lower R_{ct} value of surface modified samples suggested that the coating layer could protect the cathode materials very well by inhibiting side reactions with 1 M $LiPF_6$-EC/DEC electrolyte of HF corrosion.

EIS is a considerable technique to study the kinetic processes of Li^+ intercalation/deintercalation in the electrode. As mentioned above, the straight sloping line at low frequency region is linked with solid-state diffusion of Li^+ in the electrode bulk. Thus, the diffusion of Li^+ can be calculated from the formula below [40–42]:

$$D_{Li^+} = \frac{R^2T^2}{2n^4F^4A^2C_{Li^+}^2\sigma^2}$$

R represents the gas constant, T represents the absolute temperature, n stands for the number of electrons involved in the electrochemical process, F stands for Faraday constant, A represents the electroactive area. C_{Li}^+ stands for the concentration of Li^+ in the materials, σ represents the Warburg factor that can be calculated by the formula below. The diffusion coefficients of Li^+ for samples bare NCM, CVD1-NCM, CVD2-NCM, and HE-NCM are 4.76×10^{-10}, 1.27×10^{-9}, 8.25×10^{-10} and 6.91×10^{-10} cm^2 s^{-1}, respectively,

which seem to depend on the R_{SEI} and R_{ct} compared with the reported value. The diffusion coefficient of Li^+ decreases in the samples CVD1-NCM, CVD2-NCM, HE-NCM and bare NCM, at the same time, the rate performance shows the same change. It is noted that CVD1-NCM sample had the highest Li^+ diffusion coefficient which was achieved by coating with high electronic conductive carbon. Therefore, the improvement of the electronic conductivity, uniform protective layer contributes the better electrochemical performance of the conductively ultrathin carbon coated cathode materials.

4. Conclusion

We presented the green, novel, economic and controllable CVD method with sucrose as carbon source to coating NCM. By using this formula, the carbon layer has more uniform thickness and higher quality compared with the traditional HE. This way can be stretched to most low electronic conductivity materials. The acetic acid sol-gel synthesized NCM carbon coated using this formula show very high discharge capacity, extraordinary rate performance, high cycling performance. The thickness - optimized sample has a discharge capacity as high as 205 mAh g^{-1} and a discharge capacity for 104.5 mAh g^{-1} at 10 C (6s). High capacity retentions of 94.29 and 94.78% after 100 cycles for 0.1 C, respectively. The work is a promising coating method for the surface modification of $LiNi_{1/3}Co_{1/3}Mn_{1/3}O_2$, especially EV and HEV.

Acknowledgements

This work was supported by the Natural Science Foundation of China (No. 21566021 and 21766017), the Transformation of Scientific and Technological Achievements of Gansu Institutions of Higher Education (No. 2017D-04), and the Supporting Plan for Youth Innovative Talents of Longyuan.

References

[1] M.S. Islam, C.A.J. Fisher, Lithium and sodium battery cathode materials: computational insights into voltage, diffusion and nanostructural properties, Chem. Soc. Rev. 43 (2014) 185–204.
[2] S. Xiao, X. Li, W. Sun, B. Guan, Y. Wang, General and facile synthesis of metal sulfide nanostructures: in situ microwave synthesis and application as binder-free cathode for Li-ion batteries, Chem. Eng. J. 306 (2016) 251–259.
[3] S.-L. Chou, Y. Pan, J.-Z. Wang, H.-K. Liu, S.-X. Dou, Small things make a big difference: binder effects on the performance of Li and Na batteries, Phys. Chem. Chem. Phys. 16 (2014) 20347–20359.
[4] B. Scrosati, J. Garche, Lithium batteries: status, prospects and future, J. Power Sources 195 (2010) 2419–2430.
[5] S.B. Chikkannanavar, D.M. Bernardi, L. Liu, A review of blended cathode materials for use in Li-ion batteries, J. Power Sources 248 (2014) 91–100.
[6] V. Etacheri, R. Marom, R. Elazari, G. Salitra, D. Aurbach, Challenges in the development of advanced Li-ion batteries: a review, Energy Environ. Sci. 4 (2011) 3243.
[7] Y. Huang, J. Chen, F. Cheng, W. Wan, W. Liu, H. Zhou, X. Zhang, A modified Al_2O_3 coating process to enhance the electrochemical performance of $LiNi_{1/3}Co_{1/3}Mn_{1/3}O_2$ and its comparison with traditional Al_2O_3 coating process, J. Power Sources 195 (2010) 8267–8274.
[8] F. Fu, G.-L. Xu, Q. Wang, Y.-P. Deng, X. Li, J.-T. Li, L. Huang, S.-G. Sun, Synthesis of single crystalline hexagonal nanobricks of $LiNi_{1/3}Co_{1/3}Mn_{1/3}O_2$ with high percentage of exposed {010} active facets as high rate performance cathode material for lithium-ion battery, J. Mater. Chem. 1 (2013) 3860–3864.
[9] T. Mei, Y. Zhu, K. Tang, Y. Qian, Synchronously synthesized core-shell $LiNi_{1/3}Co_{1/3}Mn_{1/3}O_2$/carbon nanocomposites as cathode materials for high performance lithium ion batteries, RSC Adv. 2 (2012) 12886–12891.
[10] Q. Sa, J.A. Heelan, Y. Lu, D. Apelian, Y. Wang, Copper impurity effects on $LiNi_{1/3}Co_{1/3}Mn_{1/3}O_2$ cathode material, ACS Appl. Mater. Interfaces 7 (2015) 20585–20590.
[11] L. Peng, Y. Zhu, U. Khakoo, D. Chen, G. Yu, Self-assembled $LiNi_{1/3}Co_{1/3}Mn_{1/3}O_2$ nanosheet cathodes with tunable rate capability, Nano Energy 17 (2015) 36–42.
[12] H. Zheng, X. Chen, Y. Yang, L. Li, G. Li, Z. Guo, C. Feng, Self-assembled $LiNi_{1/3}Co_{1/3}Mn_{1/3}O_2$ nanosheet cathode with high electrochemical performance, ACS Appl. Mater. Interfaces 9 (2017) 39560–39568.
[13] W.-B. Hua, X.-D. Guo, Z. Zheng, Y.-J. Wang, B.-H. Zhong, B. Fang, J.-Z. Wang, S.-L. Chou, H. Liu, Uncovering a facile large-scale synthesis of $LiNi_{1/3}Co_{1/3}Mn_{1/3}O_2$ nanoflowers for high power lithium-ion batteries, J. Power Sources 275 (2015) 200–206.
[14] J. Lu, Q. Peng, W. Wang, C. Nan, L. Li, Y. Li, Nanoscale coating of $LiMO_2$ (M = Ni, Co, Mn) nanobelts with Li+-Conductive Li_2TiO_3: toward better rate capabilities for Li-Ion batteries, J. Am. Chem. Soc. 135 (2013) 1649–1652.
[15] H.-S. Kim, M. Kong, K. Kim, I.-J. Kim, H.-B. Gu, Effect of carbon coating on $LiNi_{1/3}Co_{1/3}Mn_{1/3}O_2$ cathode material for lithium secondary batteries, J. Power Sources 171 (2007) 917–921.
[16] F. Schipper, M. Dixit, D. Kovacheva, M. Talianker, O. Haik, J. Grinblat, E.M. Erickson, C. Ghanty, D.T. Major, B. Markovsky, D. Aurbach, Stabilizing nickel-rich layered cathode materials by a high-charge cation doping strategy: zirconium-doped $LiNi_{0.6}Co_{0.2}Mn_{0.2}O_2$, J. Mater. Chem. 4 (2016) 16073–16084.
[17] J. Li, X. He, R. Zhao, C. Wan, C. Jiang, D. Xia, S. Zhang, Stannum doping of layered $LiNi_{3/8}Co_{2/8}Mn_{3/8}O_2$ cathode materials with high rate capability for Li-ion batteries, J. Power Sources 158 (2006) 524–528.
[18] J. Song, B. Sun, H. Liu, Z. Ma, Z. Chen, G. Shao, G. Wang, Enhancement of the rate capability of $LiFePO_4$ by a new highly graphitic carbon-coating method, ACS Appl. Mater. Interfaces 8 (2016) 15225–15231.
[19] Q. Liu, L. Ren, C. Cong, F. Ding, F. Guo, D. Song, J. Guo, X. Shi, L. Zhang, Study on $Li_3V_2(PO_4)_3$/C cathode materials prepared using pitch as a new carbon source by different approaches, Electrochim. Acta 187 (2016) 264–276.
[20] S. Chen, T. He, Y. Su, Y. Lu, L. Bao, L. Chen, Q. Zhang, J. Wang, R. Chen, F. Wu, Ni-rich $LiNi_{0.8}Co_{0.1}Mn_{0.1}O_2$ oxide coated by dual-conductive layers as high performance cathode material for lithium-ion batteries, ACS Appl. Mater. Interfaces 9 (2017) 29732–29743.
[21] Y.S. Lee, W.K. Shin, A.G. Kannan, S.M. Koo, D.W. Kim, Improvement of the cycling performance and thermal stability of lithium-ion cells by double-layer coating of cathode materials with $Al(_2)O(_3)$ nanoparticles and conductive polymer, ACS Appl. Mater. Interfaces 7 (2015) 13944–13951.
[22] Y. Cho, P. Oh, J. Cho, A new type of protective surface layer for high-capacity Ni-Based cathode materials: nanoscaled surface pillaring layer, Nano Lett. 13 (2013) 1145–1152.
[23] R. Tian, H. Liu, Y. Jiang, J. Chen, X. Tan, G. Liu, L. Zhang, X. Gu, Y. Guo, H. Wang, L. Sun, W. Chu, Drastically enhanced high-rate performance of carbon-coated $LiFePO_4$ nanorods using a Green chemical vapor deposition (CVD) method for lithium ion battery: a selective carbon coating process, ACS Appl. Mater. Interfaces 7 (2015) 11377–11386.
[24] X. Hu, J. Chen, G. Zeng, J. Jia, P. Cai, G. Chai, Z. Wen, Robust 3D macroporous structures with SnS nanoparticles decorating nitrogen-doped carbon nanosheet networks for high performance sodium-ion batteries, J. Mater. Chem. 5 (2017) 23460–23470.
[25] Y. Uno, T. Tsujikawa, T. Hirai, Electrochemical properties of helical carbon nanomaterials formed on $LiCoO_2$ by chemical vapor deposition, J. Power Sources 195 (2010) 354–357.
[26] X. Sun, J. Li, C. Shi, Z. Wang, E. Liu, C. He, X. Du, N. Zhao, Enhanced electrochemical performance of $LiFePO_4$ cathode with in-situ chemical vapor deposition synthesized carbon nanotubes as conductor, J. Power Sources 220 (2012) 264–268.
[27] Y. Tang, F. Huang, H. Bi, Z. Liu, D. Wan, Highly conductive three-dimensional graphene for enhancing the rate performance of $LiFePO_4$ cathode, J. Power Sources 203 (2012) 130–134.
[28] Q. Gong, Y.-S. He, Y. Yang, X.-Z. Liao, Z.-F. Ma, Synthesis and electrochemical characterization of $LiFePO_4$/C-polypyrrole composite prepared by a simple chemical vapor deposition method, J. Solid State Electrochem. 16 (2012) 1383–1388.
[29] F. Wang, J. Yang, P. Gao, Y. NuLi, J. Wang, Morphology regulation and carbon coating of $LiMnPO_4$ cathode material for enhanced electrochemical performance, J. Power Sources 196 (2011) 10258–10262.
[30] B. Zhao, Y. Jiang, H. Zhang, H. Tao, M. Zhong, Z. Jiao, Morphology and electrical properties of carbon coated $LiFePO_4$ cathode materials, J. Power Sources 189 (2009) 462–466.
[31] C. Li, Q. Hou, S. Li, F. Tang, P. Wang, Synthesis and properties of nanostructured $LiNi_{1/3}Co_{1/3}Mn_{1/3}O_2$ as cathode with lithium bis(oxalate)borate-based electrolyte to improve cycle performance in Li-ion battery, J. Alloys Compd. 723 (2017) 887–893.
[32] B.J. Hwang, Y.W. Tsai, D. Carlier, G. Ceder, A combined computational/experimental study on $LiNi_{1/3}Co_{1/3}Mn_{1/3}O_2$, Chem. Mater. 15 (2003) 3676–3682.
[33] P. Gao, Y. Li, H. Liu, J. Pinto, X. Jiang, G. Yang, Improved high rate capacity and lithium diffusion ability of $LiNi_{1/3}Co_{1/3}Mn_{1/3}O_2$ with ordered crystal structure, J. Electrochem. Soc. 159 (2012) A506–A513.
[34] X. Zhang, W.J. Jiang, A. Mauger, Qilu, F. Gendron, C.M. Julien, Minimization of the cation mixing in $Li_{1+x}(NMC)_{1-x}O_2$ as cathode material, J. Power Sources 195 (2010) 1292–1301.
[35] J. Li, C. Cao, X. Xu, Y. Zhu, R. Yao, $LiNi_{1/3}Co_{1/3}Mn_{1/3}O_2$ hollow nano-micro hierarchical microspheres with enhanced performances as cathodes for lithium-ion batteries, J. Mater. Chem. 1 (2013) 11848–11852.
[36] A.M.A. Hashem, A.E. Abdel-Ghany, A.E. Eid, J. Trottier, K. Zaghib, A. Mauger, C.M. Julien, Study of the surface modification of $LiNi_{1/3}Co_{1/3}Mn_{1/3}O_2$ cathode material for lithium ion battery, J. Power Sources 196 (2011) 8632–8637.
[37] M.L. Marcinek, J.W. Wilcox, M.M. Doeff, R.M. Kostecki, Microwave plasma chemical vapor deposition of carbon coatings on $LiN_{i1/3}Co_{1/3}Mn_{1/3}O_2$ for Li-Ion battery composite cathodes, J. Electrochem. Soc. 156 (2009) A48.

[38] K.M. Shaju, G.V. Subba Rao, B.V.R. Chowdari, Performance of layered $Li(Ni_{1/3}Co_{1/3}Mn_{1/3})O_2$ as cathode for Li-ion batteries, Electrochim. Acta 48 (2002) 145–151.
[39] X. Bian, Q. Fu, X. Bie, P. Yang, H. Qiu, Q. Pang, G. Chen, F. Du, Y. Wei, Improved electrochemical performance and thermal stability of Li-excess $Li_{1.18}Co_{0.15}Ni_{0.15}Mn_{0.52}O_2$ cathode material by Li_3PO_4 surface coating, Electrochim. Acta 174 (2015) 875–884.
[40] F. Wu, X. Zhang, T. Zhao, L. Li, M. Xie, R. Chen, Surface modification of a cobalt-free layered $Li[Li_{0.2}Fe_{0.1}Ni_{0.15}Mn_{0.55}]O_2$ oxide with the $FePO_4/Li_3PO_4$ composite as the cathode for lithium-ion batteries, J. Mater. Chem. 3 (2015) 9528–9537.
[41] M. Wang, M. Luo, Y. Chen, Y. Su, L. Chen, R. Zhang, Electrochemical deintercalation kinetics of $0.5Li_2MnO_3 \cdot 0.5LiNi_{1/3}Mn_{1/3}Co_{1/3}O_2$ studied by EIS and PITT, J. Alloys Compd. 696 (2017) 907–913.
[42] X. Wang, H. Hao, J. Liu, T. Huang, A. Yu, A novel method for preparation of macroposous lithium nickel manganese oxygen as cathode material for lithium ion batteries, Electrochim. Acta 56 (2011) 4065–4069.